Wave Overtopping in the UK During the Winter of 2013/14

Dominic E Reeve

Abstract The sequence of Atlantic storms experienced by the UK during the winter of 2013/14 was very unusual. They led to widespread flooding on the west and southern coastlines of the UK and caused damage to the mainline railway between Plymouth and London. In this paper, an investigation of the severity of the impacts of the storms is presented, based on reports and new computational modelling. The resulting hypothesis is that the extensive flooding and damage were due to an unusually high percentage of swell waves. The current overtopping design formulae are not best suited to bimodal seas and new research is required to provide better design guidance for such cases.

Keywords Wave overtopping · Computational modelling · Coastal flooding Bimodal seas · Extreme events

1 Introduction

Coastal flooding and erosion are the problems experienced across the globe. The causes can be inappropriate development in the coastal zone, poor design or construction and changes in physical conditions. The latter has become the focus of much recent research based on climate change predictions promulgated by the IPCC [1, 2]. If one takes the definition of climate to be the typical conditions experienced over a time window (often taken to be anything from 10 to 30 years), then the fact that climate changes over longer periods than the window is hardly surprising given our understanding of cycles of variation that have periods much greater than a few decades. It is the cause of the change and the rate of change that has exercised the IPCC, but these are not the focus of this paper. Records from many tide gauges demonstrate a rise in sea levels over the last decade or more. It is this, together with the potential for changes in the frequency and intensity of storms that represents a

D. E. Reeve (✉)
Swansea University, Swansea, Wales, UK
e-mail: d.e.reeve@swansea.ac.uk

K. Murali et al. (eds.), *Proceedings of the Fourth International Conference in Ocean Engineering (ICOE2018)*, Lecture Notes in Civil Engineering 22,
https://doi.org/10.1007/978-981-13-3119-0_2

major risk to coastal communities. In a review of the global socio-economic potential impacts of sea level rise and increased storminess, it has been argued that the projected increases in sea level could lead to a fivefold increase in the areas of coastal zones which are flooded during storms by the 2080s [3]. Indeed, recent UN research indicates that ~40% of the world's population lives within 100 km of the coast [4]. In the UK context, 40% of our manufacturing industry is situated at or close to the coast and almost 90% of our trade passes through seaports. Ensuring facilities such as ports and other infrastructure are adequately protected is crucial for ensuring continued economic prosperity and the safety of the population.

Coastal flooding occurs either because the still water level exceeds the defence crest level, or because a breach in the defence occurs that allows water to flow through a segment of the defence or because waves run up the front face of the structure and over the crest line (known as wave overtopping). Many coastal defences are designed to withstand some level of overtopping. However, under extreme conditions overtopping rates may lead to erosion of the back face leading to slumping and lowering of the crest; damage and erosion of the crest; removal of sediment and or armour units from the front face leading to slumping of the front face and/or erosion of the core and eventual breaching. Excessive wave overtopping is a major cause of breaching in coastal defences and so being able to predict overtopping rates under extreme conditions is an important design requirement. However, wave overtopping can lead to flooding, even if no damage occurs to the structure, if inadequate account has been taken of drainage capacity. In these cases, overtopping water gradually accumulates behind the structure, pooling, thus creating a flooding hazard. Water overtopping a defence will have appreciable momentum and often flow from an overtopping can penetrate 10s of metres inland.

Key elements of wave overtopping are illustrated in Fig. 1. The overtopping rate, measured in $m^3/s/m$-run of defence, is often denoted by 'q'. The distance between the undisturbed water level and the crest of the defence is termed the freeboard, R_c.

Overtopping usually occurs under conditions where there is a combination of large waves and high water levels [6, 7]. Such conditions are common during mid-latitude storms in which low surface pressure and strong winds act to generate surge and waves. Empirical formulae for predicting wave overtopping under these conditions have been developed by a number of researchers [7–10]. Most of the formulae relate

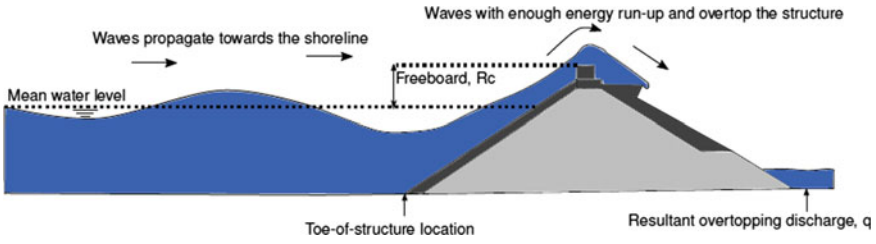

Fig. 1 Illustration wave overtopping and key quantities (adapted from [5])

a non-dimensionalised overtopping rate to the freeboard through an exponential or power law. For example, Owen's formula reads [11]:

$$Q = a\mathrm{e}^{-bR/r} \tag{1}$$

where $Q=q/(gH_sT_m)$, $R=(R_c/H_s)\sqrt{(s_m/2\pi)}$, H_s is the significant wave height at the toe of the sea wall, T_m is the mean zero crossing period at the toe of the sea wall, s_m is the notional wave steepness (H_s/deep water wavelength), r is a roughness coefficient which varies from 0 to 1 depending on the material properties of the front face of the sea wall, and parameters a and b are empirically determined and vary with the geometry of the sea wall. Empirical formulae such as Eq. (1) are used in the design of coastal defences around the world and provide effective estimates under storm wave conditions.

However, the formulae are based on wave conditions best described as wind seas, with a unimodal frequency spectrum and relatively low peak wave period, and are not representative of conditions with a significant swell component. In an investigation of the applicability of empirical formulae to describe overtopping by swell waves [12], the formulae of Owens, Hedges and Reis and Van der Meer [7–9] were compared against physical modelling results of wave overtopping under bimodal wave conditions. Hawkes [12] found that Owen's formula over predicts the mean overtopping rate by a factor of as much as 5. As Owen's formula depends on wave period and was based on wind sea conditions only, this behaviour is perhaps not unsurprising. Both the Van der Meer and Hedges and Reis formulations account for the dependence of wave overtopping on wave breaker type, with separate formulae for plunging and surging waves, and were found to give better predictions than Owen's formula. However, over the range of foreshore slopes used by [12] the Van der Meer formula was found to give an underestimate of overtopping and it was concluded that none of the three formulae provided adequate predictions of overtopping under swell wave conditions.

In many places around the world, coastal storm wave conditions cannot always be described by unimodal, wind sea spectra, such as the Pierson–Moskowicz or JONSWAP spectra [13]. As will emerge in the following sections, when unusual meteorological conditions occur the presence of a significant swell component can alter the expected overtopping volumes and cast doubt on the efficaciousness of traditional overtopping formulae.

The structure of this paper is as follows. In Sect. 2, the meteorological conditions that affected the UK during the winter of 2013/2014 are described together with the features that made this an unusual season. Section 3 describes the computational model used to simulate wave overtopping. Section 4 presents a selection of results from the modelling, and the paper concludes with a brief discussion or the results and scope for future research.

2 The Winter of 2013/2014

From December 2013 to January 2014, the UK experienced a sequence of storms typical of the season. From late January to mid-February 2014, a succession of six major storms passed over the UK, separated by intervals of 2–3 days. The UK Met Office now names major storms, and in this period, there were four named storms. Taken individually, the first two storms were notable but not exceptional for the winter period. However, the later storms from early to mid-February were much more severe. Overall, the period from mid-December 2013 to mid-February 2014 saw at least 12 major winter storms, and when considered overall, this was the stormiest period of weather the UK has experienced for at least 20 years [14].

Storm Petra which hit the UK on 5 February 2014 caused considerable damage along the coast, particularly in mid-Wales, Devon and Cornwall. Estimating the severity of storms is not straightforward. Meteorological measurements tend to focus on surface pressure and wind speeds while operational flood agencies emphasise water level and wave height. Based on a comparison of measured and modelled wave heights, [15] argued that the wave conditions during this period were the most energetic for about 60 years. A slightly different perspective was provided by [14] who noted that although no individual storm could be regarded as exceptional, the clustering and persistence of the storms was highly unusual. Further, the tracks of the storms fell at uncharacteristically low latitude, leading to severe gales along the south and west coasts of the UK where the bulk of the ocean wave energy was directed. Peak wave periods were very long so individual waves contained more energy than normal storm waves and hence were able to inflict greater damage and flooding.

A summary of the damage experienced during the period around Storm Petra is given in Table 1. There was widespread flooding in Cornwall on 2 February 2014. Extensive damage to sea walls occurred along the south Devon coast on 4 February 2014, leading to the closure of the mainline London to Plymouth railway service for several days and severe restrictions on timetabled services for several months.

The total economic damage for England and Wales during the winter period was estimated to be between £1000 million and £1500 million, including the damage associated with fluvial and groundwater flooding [16]. Detailed meteorological analysis of the storms and their impacts can be found in [14].

3 Computational Model

To investigate what impacts a bimodal wave state might have on wave overtopping of coastal structures, we adopted the NEWRANS model [17], in which a ‘numerical flume’ can be created to simulate the fluid dynamical processes. Here, we provide a summary description of the model and the interested reader is referred to [17] for further details. The model solves the Reynolds-averaged Navier–Stokes equations on a fixed rectangular mesh. As a result, a set of equations are defined for the mean flow

Table 1 Locations and extent of damage during Storm Petra

Date	Location	Observed damage	Cost estimate
2/2/14	Looe Bay	Flooding	N/A
	Perranporth	Flooding	N/A
	Bude	Flooding	N/A
	Portreath	Flooding	N/A
	Trevone, Padstow	Wall collapse	N/A
	Newquay	Sea wall damage/Road collapse	N/A
4/2/14	Dawlish	Sea wall collapse	£35 million
	Newton Abbott/Paignton	Sea wall collapse	N/A
	Newton Abbott/Plymouth	Sea wall collapse	N/A

containing contributions from the fluctuating turbulent flow. To describe the turbulent flow, the model is coupled with a second-order k-ε turbulence closure model, where k is the turbulent kinetic energy and ε is the turbulent dissipation. It incorporates a volume-of-fluid (VOF) surface capturing scheme to allow for accurate simulation of large surface deformations during wave breaking and overtopping. The model simulates a single liquid phase (water) and does not capture bubble formation. The model has been validated through a range of applications to wave breaking, run-up and overtopping [17–19].

A crucial element of the modelling is proper creation of the wave conditions. A bimodal wave condition represents a significant challenge because not only are the waves random but there is a widespread of wave periods. There are two established methods for generating waves: the wave paddle method which emulates the paddle movement in a laboratory wave tank; and the internal mass source. For the wave paddle method, waves are generated from the boundary of the domain and propagate away from the boundary in one direction. The velocity and free surface value are specified on the wave boundary. Reflected waves that reach the paddle position can degrade the wave generation signal due to re-reflection from the wave generation boundary. In addition, the method can introduce mass to the domain through Stokes' drift included in the boundary conditions. A scheme to avoid these problems was presented by [20]. The internal mass source function method, developed by [21], generates waves within the domain causing waves to propagate away from the generation area from either side. An important consideration when using the internal mass source method is the size and positioning of the internal mass source: if the source region is placed too deep below the surface, the wave will be too small; if placed too close to the surface, the waves generated will be too steep.

Both methods were tested. A key measure of the bimodality of the waves is the percentage of swell, P_{sc}, defined as the percentage of energy in the swell component

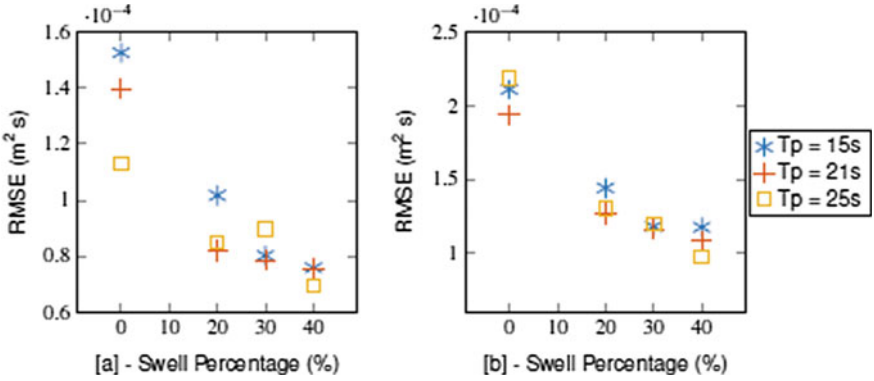

Fig. 2 RMSE between observed and simulated $S(f)$ for (left) wave paddle and (right) internal mass source (adapted from [5])

of the energy density spectrum, $S(f)$. To compare the accuracy of the two wave generation methods, the model wave distributions were compared against a sequence of experiments described in [22] for which bimodal conditions were created for a range of T_p and P_{sc}. The waves were predominately intermediate water waves ($0{:}05 < d = L < 0{:}75$). The spectra from the simulations and experiments are compared at a point a short distance from the wave generator. The root mean square error (RMSE), between the simulated and experimental spectra (averaged over frequency), was calculated for both internal mass source and paddle methods. Results are shown in Fig. 2 which indicates that the paddle method produces a more accurate representation of the desired spectrum. The RMSE reduces for both methods as P_{sc} increases.

The wave paddle wave generation method was chosen for the main set of simulations. A more detailed discussion of the creation of bimodal wave conditions in the computational flume is given in [5, 23].

4 Results

In order to specify a bimodal spectrum that had the desired combination of wave characteristics (e.g. H_{m0}, T_p, $T_{m\text{-}1,0}$, T_{m02}), an iterative semi-automated procedure was developed to form the wave train. This was used, for example, to define a sequence of spectra which had constant energy and integrated wave period ($T_{m\text{-}1,0}$), but varying percentages of swell such as shown in Fig. 3. The peak period, T_p, is defined as the period at which the spectrum attains its maximum value. This can vary quite rapidly and is hence not a reliable measure of the energy of the sea state, although it is used in some overtopping formulae. T_{m02} has an approximate equivalence to the mean zero up-crossing period familiar in time-domain analysis, while $T_{m\text{-}1,0}$, sometimes known as the mean energy period, is the mean wave period with respect

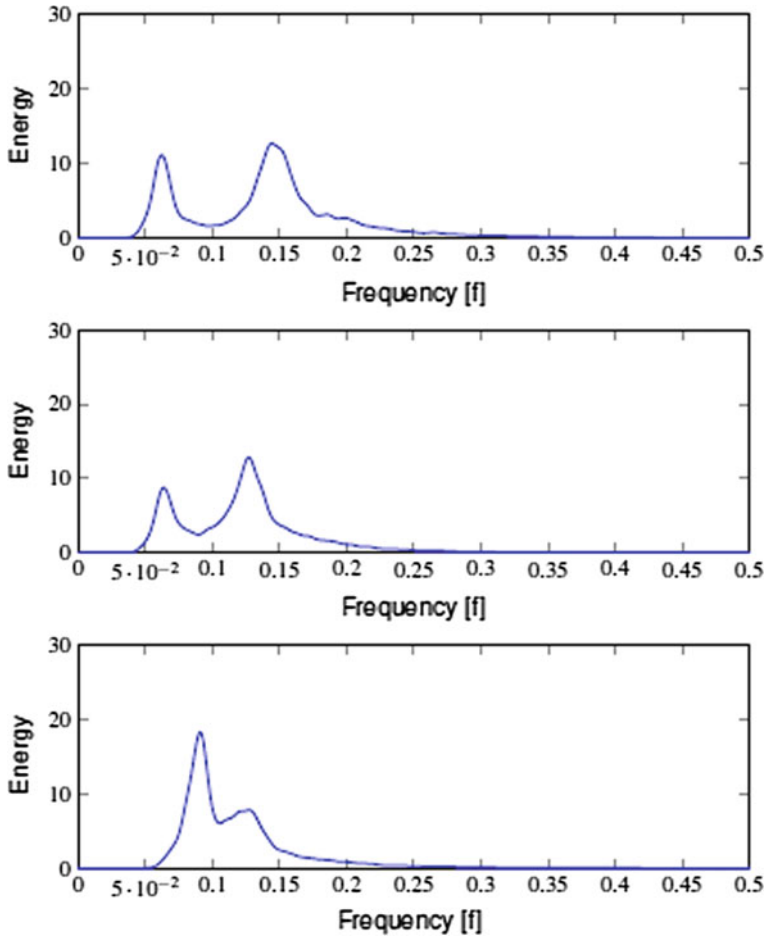

Fig. 3 Example spectra for defined $T_{\text{m-1,0}} = 12$ s for varying P_{sc} with a constant total energy content. $P_{\text{sc}} = 20$, 50 and 80% from top panel to bottom panel (adapted from [5])

to the spectral distribution of energy and may be thought of as the period of the regular wave that has the same significant height and power density as the sea state under consideration. Both T_{m02} and $T_{\text{m-1,0}}$ are used in recent overtopping formula, and [7] argues that $T_{\text{m-1,0}}$ places more weight on energy at lower frequencies and is therefore more appropriate for describing overtopping due to bimodal sea states.

Experimental studies of overtopping under bimodal seas are scarce. However, results of some experiments can be found in [12, 24]. The bimodal sea conditions consisted of two superimposed JONSWAP spectra, with each spectrum defined by its significant wave height, H_{s}, and peak wave period, T_{p}. The model was validated against three experiments for which wave conditions had equal energy, with a wind sea peak period at 7 s coupled with swell at 11, 14 and 19 s. The computational

model was able to replicate the observed experimental overtopping discharges very well for Iribarren numbers above 2.2 [5]. However, the model under-predicted when little overtopping discharge was observed and when a low Iribarren number was observed. This is likely to be due to difficulties encountered by the volume-of-fluid method capturing small overtopping volumes, as well as the representation of the turbulent wave breaking processes for low Iribarren number.

An extensive set of computational experiments was devised in order to explore how mean overtopping rates varied with swell percentage, freeboard, and measures of wave period (T_p, T_{m02} and $T_{m-1,0}$). Some of the representative results are shown here. The wave conditions were defined by their total energy, swell percentage, P_{sc}, and mean wave period, T_{m02}. All wave conditions had equal energy, as defined by the integral of their spectra. The wave sequences for each case were derived with a high energy content, representative of conditions during the storms at Dawlish. Wave sequences were created that had equal energy but varying mean wave period and associated swell percentage.

Figure 4 shows the mean overtopping rate plotted against mean wave period for a range of swell percentages. Results from individual computations are shown as dots with the line of best fit showing the averages observed for the given swell percentage. Except in the cases with the largest percentage of swell, there is a clear increase in overtopping rate with mean period. Also clear is the reduction in the scatter of computed overtopping rates as the mean wave period increases. This suggests swell percentage has a greater effect on mean overtopping discharge in sea states for which T_{m02} is relatively small, representative of wind sea conditions.

Figure 4 also shows that for a fixed value of $T_{m02,}$ overtopping rates increase with increasing swell percentage. Again, this sensitivity is strongest for conditions with relatively low swell percentage (P_{sc} between 10 and 30%), reducing as the swell percentage increases.

Figure 5 shows mean overtopping rates as a function of swell percentage for $T_{m-1,0}$ = 4, 7 and 10 s. There is a clear increase in overtopping rate with swell percentage,

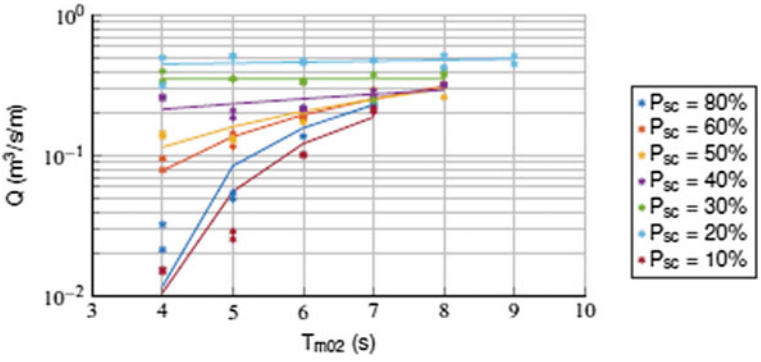

Fig. 4 Mean overtopping rate plotted against mean wave period (T_{m02}), for varying P_{sc} with a constant total energy content (adapted from [5])

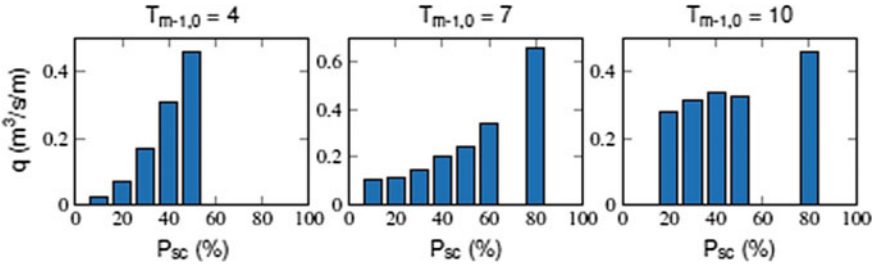

Fig. 5 Mean overtopping rate plotted against swell percentage for $T_{m\text{-}1,0} = 4$, 7 and 10 s (left, middle and right panels, respectively) (adapted from [5])

which is especially noticeable for the smaller periods; but influence of swell percentage is still observed for the higher mean wave periods. Potentially the most important swell percentage is 20–40% due to the increased rate in overtopping discharge associated with these swell percentages. The influence of swell percentage on $T_{m\text{-}1,0}$ is an important finding as $T_{m\text{-}1,0}$ is the recommended parameter used for overtopping discharge under bimodal conditions. The results in Fig. 5 demonstrate that for a fixed value of $T_{m\text{-}1,0}$, overtopping discharge can still vary with swell percentage.

5 Discussion and Conclusions

The storms of winter 2013/2014 experienced by the west coast of the UK led to extensive flooding and damage. Analyses of the storm conditions indicated that while individual storms were not exceptional, the clustering and storm tracks were unusual. In particular, wave spectra along the south and south-west UK coastline highlighted the increased frequency of bimodal conditions. Reliable methods for predicting wave overtopping under bimodal and swell conditions have been constrained by limitations of the empirical methods and by a lack of suitable data.

In this paper, we have described a computational investigation aimed at addressing some of these limitations. The study is based on an adaptation of a well-established RANS-VOF model to examine the influence of swell and bimodal wave conditions on overtopping.

The selection of results shown here demonstrates that the wave overtopping rate is strongly dependent on the swell content of the wave energy spectrum, with greatest sensitivity evident for swell percentages in the range 20–40%. Further, the overtopping rates show sensitivity to swell percentage when either T_{m02} or $T_{m\text{-}1,0}$ is held constant. This suggests that the guidance provided in [7] regarding the applicability of empirical overtopping formulae to bimodal conditions is potentially overstated. This is further supported by a study of the impacts of these storms at a site in Wales [25], which illustrated how current overtopping formula underestimated wave overtopping rates.

Our study confirms the sensitivity of overtopping rates to the shape of the wave spectrum (not just its integral) and points to a requirement to include this factor in empirical formula. Our understanding of overtopping in bimodal sea states is incomplete and further research is required, given the damaging nature of their impacts.

Acknowledgements The author would like to acknowledge the contributions of Dr. Daniel Thompson, particularly for the figures.

References

1. IPCC WG1 (2007) Climate change 2007: the physical science basis. Contribution of the Working Group I to the Fourth Assessment Report of the Intergovernmental Panel on Climate Change, Cambridge University Press, Cambridge, UK, 940 pp
2. IPCC WG2 (2007) Climate change 2007: impacts, adaptation and vulnerability. Contribution of the Working Group II to the Fourth Assessment Report of the Intergovernmental Panel on Climate Change. Cambridge University Press, Cambridge, UK, 1000 pp
3. Nicholls RJ, Cazenave A (2010) Sea level rise and its impact on coastal zones. Science 328(5985):1517–1520
4. SEDAC (2011) Percentage of total population living in coastal areas, Technical report, United Nations. URL: http://sedac.ciesin.columbia.edu/es/papers/Coastal_Zone_Pop_Method.pdf, (Accessed 4/1/18)
5. Thompson DA (2017) Computational investigation into the effects of bimodal seas on wave overtopping. Ph.D. thesis, Swansea University, 263 pp
6. Pugh D, Woodworth P (2014) Sea-level science: understanding tides, surges, tsunamis and mean sea-level changes. Cambridge University Press, Cambridge
7. Van der Meer J, Allsop N, Bruce T, De Rouck J, Kortenhaus A, Pullen T, Schüttrumpf H, Troch P, Zanuttigh B (2016) EurOtop 2016: manual on wave overtopping of sea defences and related structures. An overtopping manual largely based on European research, but for worldwide application. Technical report. URL: http://www.overtopping-manual.com (Accessed 4/1/18)
8. Owen MW (1980) Design of seawalls allowing for wave overtopping, HR Wallingford Report EX924, UK
9. Hedges T, Reis M (1998) Random wave overtopping of simple sea walls: a new regression model. Proc Inst Civ Eng Water Marit Energy 130:1–10
10. Steendam GJ, Van Der Meer JW, Verhaeghe H, Besley P, Franco L, Van Gent MR (2004) The international database on wave overtopping. In: Coastal engineering 2004—proceedings of the 29th international conference. World Scientific Publishing Co. Pte. Ltd., Singapore, pp 4301–4313. URL: http://eproceedings.worldscinet.com/9789812701916/9789812701916_0347.html (Accessed 4/1/2018)
11. Environment Agency: Overtopping of Seawalls. R&D Project Record W5/006/5, 1999. 132p. https://www.gov.uk/government/uploads/system/uploads/attachment_data/file/290227/sprw5-006-5-e-e.pdf (accessed 4/1/2018)
12. Hawkes P (1999) Mean overtopping rate in swell and bimodal seas. Proc Inst Civ Eng Water Marit Energy 136:235–238
13. Reeve DE, Chadwick AJ, Fleming CA (2012) Coastal engineering: processes, theory and design practice, 2nd edn. Spon Press, 514 p
14. Masselink G, Castelle B, Scott T, Dodet G, Suanez S, Jackson D, Floc'h F (2016) Extreme wave activity during 2013/2014 winter and morphological impacts along the Atlantic coast of Europe. Geophys Res Lett 43:2135–2143. https://doi.org/10.1002/2015gl067492
15. UK Met Office/Centre for Ecology and Hydrology: The recent storms and floods in the UK, February 2014, 29 p. http://nora.nerc.ac.uk/id/eprint/505192/1/N505192CR.pdf (accessed 4/1/2018)

16. Environment Agency: The costs and impacts of the winter 2013 to 2014 floods. Report SC140025/R1, 2016, 275 p. https://www.gov.uk/government/uploads/system/uploads/attachment_data/file/501784/The_costs_and_impacts_of_the_winter_2013_to_2014_floods_-_report.pdf (accessed 4/1/18)
17. Lin P, Liu PL-F (1998) A numerical study of breaking waves in the surf zone. J Fluid Mech 359:239–264
18. Jones DK, Zou Q, Reeve DE (2013) Computational modelling of coastal flooding caused by combined surge overflow and wave overtopping on embankments. J Flood Risk Manag 6(2):70–84. https://doi.org/10.1111/j.1753-318x.2012.01155.x
19. Soliman A, Reeve DE (2003) Numerical study for small freeboard wave overtopping and overflow of sloping sea walls. In: Proceedings of coastal structures 2003, ASCE, Portland, USA, pp 643–655
20. Torres-Freyermuth A (2007) Estudio de la Hidrodin'amica de la Zona de Rompientes mediante ecuaciones tipo RANS. Ph.D. thesis, Universidad de Cantabria, Santander
21. Lin P, Liu P (1999) Internal wave-maker for Navier-Stokes equations models. J Waterw Port Coast Ocean Eng 125(4):207–215
22. Polidoro A, Pullen T, Powell K (2016) Modelling shingle beaches in bimodal seas—development and application of Shingle-B. Technical Report December, HR Wallingford. URL: http://www.channelcoast.org/shingleb/
23. Thompson DA, Karunarathna H, Reeve DE (2016) Numerical simulation of bimodal seas: a comparison between wave generation methods. Water Sci Eng 9(1):p3–13
24. Coates TT, Jones RJ, Bona PFD (1998) Wind/swell seas and steep approach slopes: technical report on wave flume studies. Technical Report TR 24, HR. Wallingford
25. Thompson DA, Karunarathna H, Reeve DE (2017) Modelling extreme wave overtopping at Aberystwyth Promenade. Water 9:663–679. https://doi.org/10.3390/w9090663